

Microwave synthesis and characterization of nanocrystalline Mn-Zn ferrites

Surender Kumar^{1*}, Tukaram J. Shinde², Pramod N. Vasambekar³

¹Department of Physics, Pandit Anant Ram Sanatan Dharam College, Baroh 176054, India

²Department of Physics, KRP Kanya Mahavidyalaya, Islampur 415409, India

³Department of Electronics, Shivaji University, Kolhapur 416004, India

*Corresponding author. Tel: (+91) 9816383716; E-mail: surender.postbox@gmail.com

Received: 19 October 2012, Revised: 22 November 2012 and Accepted: 06 December 2012

ABSTRACT

Powder diffraction, Fourier transform infrared spectroscopy and scanning electron microscopy were used to characterize the spinel structure of nanocrystalline Ferrites with composition $Mn_{1-x}Zn_xFe_2O_4$ ($x = 0.2, 0.4, 0.6$ and 0.8) prepared by oxalate coprecipitation technique and followed by microwave heating of precursors. Effect of composition on the lattice constant, x-ray density, crystallite size was studied. Crystallite size and x-ray density increases with increase in Zinc content. The face centered cubic spinel structure has undergone deviation from ideality. A correlation exists between splitting of infrared absorption bands and lowering of composition dependent crystalline symmetry. This preparation technique could be used for synthesis of materials which use microwave transparent precursors. Copyright © 2013 VBRI press.

Keywords: Ferrites; microwave synthesis; XRD; FTIR; SEM.



Surender Kumar received B.Sc. (Honours) and M.Sc. degree in Physics from University of Delhi in India in 1996 and 1998 respectively. He is Assistant Professor and head in the Department of Physics, Pt. Anant Ram Sanatan Dharam College, Baroh in India. He is pursuing Ph.D. in the department of Electronics, Shivaji University, Kolhapur in India. His field of research is microwave synthesis of multi-component nanocrystalline oxides and the studies of their electrical and magnetic properties. His research interest also includes gas, humidity sensors and electrical switching in nanocrystalline materials.



Pramod N. Vasambekar obtained M.Sc. and Ph.D. in Physics from Shivaji University, Kolhapur in India in 1986 and 1995 respectively. He is presently working as an Professor in Department of Electronics, Shivaji University. During his research carrier, he is involved in the synthesis and characterization of solid state material for microwave and communication electronics. Dr. Vasambekar published 65 research papers in scientific journals and conferences on synthesis of ferrites and their applications as gas and humidity sensor, electrical switching and microwave absorbing materials.



Tukaam Jaysing Shinde received his B.Sc. degree in Physics from Krishna Mahavidyalaya, shivanager (Shivaji University, Kolhapur) in 1988. His M.Sc., M.Phil and Ph. D. degrees were obtained from Shivaji University, Kolhapur(India) in 1990, 2001 and 2010. He joined at A. S. C. College, Lonand as lecturer in physics from 1990. Presently he is working as Associate professor in physics department at K.R.P. Kanya Mahavidyalaya, Islampur. He has published 23 research articles in various

scientific journals and presented paper at national and international conferences. His research activities have been focused in field of ferrite electromagnetic wave and gas sensors.

Introduction

Ferrites are electrically semiconducting and structure sensitive ferrimagnetic oxides [1, 2]. Metal cations occupy in octahedral and tetrahedral sites formed by Oxygen anions in a face centered cubic (fcc) spinel structure. The oxygen anions dominate the presence of cations in fcc lattice. They form a perforated enclosure for metallic cations present in tetrahedral and octahedral sites; thereby imposing a cloud of restrictive dominance over metallic behavior of cations. So the metallic cations are not independent in the spinel lattice and hence the oxygen anions regulate electrical and magnetic properties of ferrites. The scope of regulation depends on the type of site, cation and its valency.

Ferrites are prepared by various methods such as ceramic [3], coprecipitation [4], citrate precursor [5], hydrothermal [6], layered precursor [7], shock wave treatment [8], sol-gel [9], combustion [10], thermal decomposition [11], [12]. Of these, ceramic method is commercially most successful method for ferrite production. However, it is time consuming [4] and energy intensive [13]. It leads to poor compositional [13, 14], density and size controls [14] and introduces chemical inhomogeneities, impurities [13], [15], lattice strains during ball milling and grinding leading to non-reproducible products [16]. The co-precipitation is a simple and effective method for preparation of ferrites at nanoscale. It is a low temperature process and provides good control over crystallite size [17], improves homogeneity of cation distribution, lowers porosity and particle size distribution. The co-precipitation method leads to intimate mixing of starting materials on ionic level so that crystallization can occur at low temperatures [15]. In recent past nanocrystalline ferrites prepared by coprecipitation technique have generated significant interest as compared to their bulk counterparts. At nanolevel ferrites exhibit novel phenomena and hence potential for innovative technological applications. The reduction in the size of the nanoparticles leads to increase in relative surface area. The quantum size effect and the large surface area of nanoparticles dramatically change some of the magnetic properties and exhibit superparamagnetic phenomena and quantum tunneling of magnetization, because each particle behaves as single magnetic domain [18].

Mn-Zn ferrites are very important soft magnetic materials because of their high initial magnetic permeability, saturation magnetization, electrical resistivity and low power losses. These materials are extensively used as inductors, transformers, antenna rods, loading coils, deflection yokes, choke coils, recording heads, magnetic amplifiers, electromagnetic interference devices (EMI), power transformers and splitters. Moreover, Mn-Zn ferrites are very important in biomedicine as magnetic carriers for bioseparation, enzymes and proteins immobilization. Recently, with the development of high frequency, low power miniaturized electronic devices; special focus has been placed on preparation of high performance Mn-Zn ferrite powders [19, 20].

In recent times microwave synthesis has emerged as an efficient technique for synthesis of new materials [21-23]. It is cost effective, time saving and environment friendly technique. When exposed to microwave radiations,

materials may reflect, absorb or remain transparent. The absorption of microwave radiation causes rise in temperature of material due to dielectric heating [24]. Microwave heating is low on energy consumption as compared to conventional furnace. This is because volumetric heating rapidly converts precursors into ferrites. Thus, microwave heating is an energy efficient method for rapid conversion of co-precipitated precursors into ferrite powders. This work aims to prepare nanocrystalline ferrites by combining oxalate coprecipitation technique and microwave heating.

Experimental

Materials synthesis

Nanocrystalline soft ferrites with general formula $Mn_{1-x}Zn_xFe_2O_4$ ($x=0.2, 0.4, 0.6$ and 0.8) were synthesized by oxalate co-precipitation technique and microwave sintering. Manganese sulfate monohydrate ($MnSO_4 \cdot H_2O \geq 99\%$, Merck), Iron (II) sulfate heptahydrate ($FeSO_4 \cdot 7H_2O \geq 99\%$, Merck), Zinc sulfate heptahydrate ($ZnSO_4 \cdot 7H_2O \geq 99\%$, Merck) were used as starting materials. All metal sulfates were dissolved in double distilled water at room temperature. The concentration of metal ions was kept at 1.5 moles per liter. Aqueous solution of precipitating agent was prepared by dissolving seven parts by weight of water to one part of di-ammonium oxalate monohydrate ($(NH_4)_2C_2O_4 \cdot H_2O$, Guaranteed reagent, Merck). The temperature of metals ion solution was maintained at 45 °C by using magnetic stirrer and hot plate. The aqueous solution of Di-ammonium oxalate monohydrate was rapidly added to the sulfate solutions under continuous stirring. Addition of precipitating agent was stopped when the pH of metal ion solution undergoing precipitation reached 3.5. The stirring was continued for 30 minutes. Bright yellow precipitate was allowed to settle in the beaker and supernatant liquid was poured off. Excess ammonium oxalate and sulfate contaminant in the precipitates were washed by using distilled water. Barium chloride test was used to confirm absence of sulfate ions in the precipitates. The precipitates were dried in an oven at 100° C for 8 hours. The dried precipitate was poured in quartz crucible. Thereafter, crucible was placed in a cylindrical cavity created inside a high alumina (alumina~80 %). The gap between quartz crucible and wall of the cavity was filled with aluminum powder. Since the metal oxalates in the precipitate are poor absorbers of microwave radiation; it was necessary to use microwave susceptor for heating. The aluminum powder is a moderate absorber of microwave radiations. Hence it was preferred over strong absorbers of microwave radiations such as Silicon carbide or transition metal oxide. The high alumina brick containing susceptor (aluminum powder), crucible with dried precursor was placed on the turn table of commercial microwave oven (ONIDA, 25XL Power convection) operated at frequency 2.45 GHz and maximum output power 900 Watts. The oven was operated at 60% of optimum power for 630 seconds to take the temperature of precursors to 450 °C. Brick was immediately brought out of the oven and allowed to cool.

Materials characterization

The XRD patterns of samples were recorded in the scattering range (2θ) of 10° - 80° , scan rate of 0.05° per second and a primary beam power of 40kV, 30mA using a Bruker AXS D8 Advance X-ray diffractometer with Cu- K_α radiation ($\lambda=1.54058 \text{ \AA}$). FTIR spectra were recorded in the range 350 - 800 cm^{-1} on Perkin Elmer, spectrum one spectrophotometer using KBr pellet (1mm thickness, 1:100 ratio of KBr to the specimen) method. The microstructure and morphology of nanocrystalline ferrites were investigated by scanning electron microphotographs under JEOL JSM-6610LV scanning electron microscope.

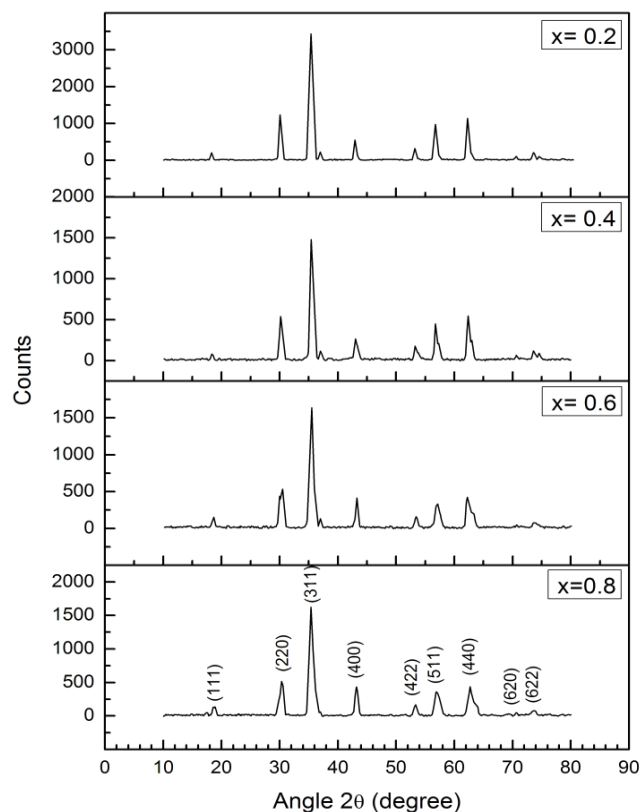


Fig.1. X-ray diffraction pattern $Mn_{1-x}Zn_xFe_2O_4$.

Results and discussion

Coprecipitation is a simple method and is widely used in industry and research for preparation of complex oxides. Atomic mixing of the constituents in chemical coprecipitation allows preparation of materials at low temperatures [25]. Oxalate coprecipitation technique prepares precursors which are insoluble in water and hence this work allows preparation of stoichiometric spinel ferrites. The process involves the simultaneous occurrence of nucleation, growth, coarsening and/or agglomeration [26]. Thereafter; the precipitates are washed, filtered and dried for heat treatment in order to prepare the final product. Conventionally conversion of co-precipitated precursors into spinel ferrites requires heat treatment in a furnace for hours. Heating in a furnace is not only time consuming but also energy intensive. Whereas, microwave heating has inherent advantages. The dielectric constant or complex permittivity ($\epsilon = \epsilon' - j\epsilon''$) plays a vital role in

microwave heating. The complex permittivity of a material is a measure of the ability of a material to absorb and store dielectric potential energy. The real part (ϵ') represents penetration of microwaves into material and loss factor (ϵ'') indicates ability of material to store energy. The parameter $\tan \delta = \epsilon''/\epsilon'$, the ability of material to convert absorbed energy into heat, is the most important property in microwave processing. Higher $\tan \delta$ causes rapid heating. Many Metal oxides couple strongly with microwave radiations whereas metal powders are moderate absorbers of microwave radiations [24]. Metal powders have moderate value of $\tan \delta$ hence they can be used for controlled heating of materials.

The peaks in XRD patterns (Fig. 1) illustrate the characteristic peaks of single phase cubic spinel structure.

Peak intensity is indicative of high degree of crystallinity of prepared ferrites. Interplaner distances (d_{hkl}) were calculated by using Bragg's law. The lattice constant ($a = d_{hkl} \sqrt{h^2 + k^2 + l^2}$) and average crystallite size (D) were calculated from the most intense (311) peak of the diffraction pattern,

$$D = \frac{0.94\lambda}{\beta \cos \theta} \quad (1)$$

where β is full width at half maximum (FWHM) of (311) peak. X-ray density (dx) of the ferrite samples was calculated using the expression-

$$d_x = \frac{ZM}{Na^3} \quad (2)$$

where M is the molecular weight of ferrite sample, N is Avogadro's number and Z is number of molecules per unit cell. For spinel cubic structure Z is 8. The lattice constant (a), Interplaner spacing (d) for (311) planes, X-ray density (dx) and crystallite size (D) are exhibited in Table 1.

Table 1. Effect of composition on lattice Constant, crystallite size and x-ray density for $Mn_{1-x}Zn_xFe_2O_4$ system.

X	Position of (311) peak (degree)	Interplaner spacing(d) (Å)	Lattice Constant (nm)	Crystallite Size (nm)	X-Ray density (g/cm^3)
0.2	35.35	2.54	8.41	11.51	5.19
0.4	35.52	2.53	8.38	14.62	5.30
0.6	35.45	2.53	8.40	15.50	5.32
0.8	35.36	2.54	8.41	29.80	5.33

The cation distribution in ferrites governs the lattice constant. The cations with variable ionic radii can expand or contract the unit cell due to their occupation of available interstitial sites. In bulk Mn-Zn ferrites, zinc ions occupy tetrahedral sites (A-sites). However in nanoregime Zn^{2+} also

occupy octahedral B sites. On octahedral site (B-site) the ionic radius of Zn^{2+} is substantially higher (0.074 nm) than that on tetrahedral site (0.060 nm). For lowest content of zinc ($x=0.2$), the lattice constant is larger due to substantial occupation of high spin Mn^{2+} ions (ionic radius = 0.083 nm) on octahedral sites. For $x=0.4$, for increased Zn content, the lattice constant is therefore reduced. The gradual rise in zinc content (x), thereafter, leads to increased occupation of octahedral sites by Zn^{2+} ions. The higher ionic radius of Zn^{2+} ions on octahedral sites increased lattice parameter for $x=0.6$ and $x=0.8$ since unit cell had to expand. The presence of Mn^{3+} is ruled out since oxidation of Mn^{2+} requires calcination above 500 °C in air [27].

Infrared spectroscopy is used to determine local symmetry in crystalline solids, ordering phenomena in spinels, presence or absence of Fe^{2+} ions, force constants and elastic moduli of ferrites [28]. Waldron classified the vibrations of the unit cell of cubic spinel. High wavenumber absorption band at ν_1 is caused by stretching vibrations of the tetrahedral metal-oxygen bond, and low wavenumber absorption band ν_2 is caused by metal-oxygen vibrations on octahedral sites [29]. FTIR spectra is shown in Fig. 2; In addition to primary bands (ν_1 and ν_2) of Ferrites, the spectra contain additional bands representing splitting of primary absorption bands ν_1 and ν_2 in ferrites. Table 2 illustrates the wavenumbers corresponding to various absorption bands. The splitting of ν_1 appears as high intensity band (ν_{1sp}) and another low intensity band (ν_{1sh}) due to lowering of symmetry of cubic crystalline structure of spinel ferrites. The splitting of ν_2 attributed to Jahn teller distortion at octahedral site, led to additional absorption band (ν_{2sp}). The primary band (ν_1) varies from 564.30 cm^{-1} to 551.13 cm^{-1} with increasing zinc content, whereas ν_2 remains unaffected with variation in composition.

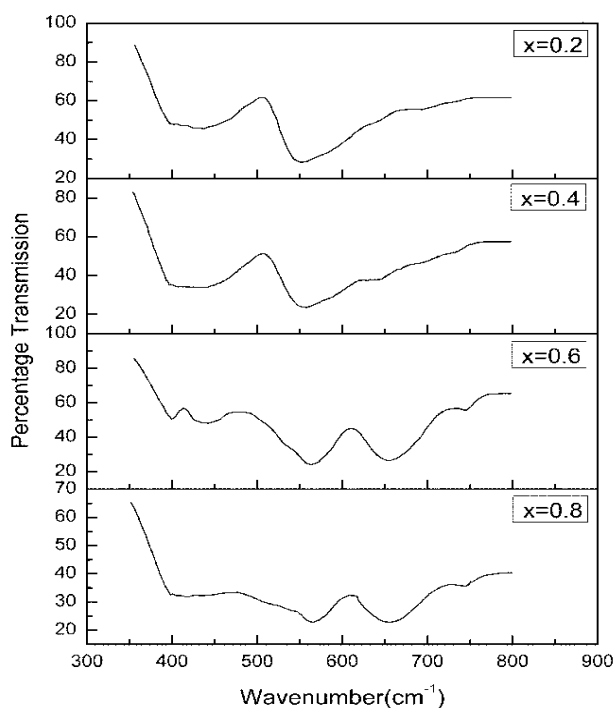


Fig. 2. FTIR absorption spectra for $Mn_{1-x}Zn_xFe_2O_4$.

Table 2. The FTIR absorption bands(in cm^{-1}) for $Mn_{1-x}Zn_xFe_2O_4$.

x	Tetrahedral site		Octahedral site		
	ν_{1sh}	ν_{1sp}	ν_1	ν_2	ν_{2sp}
0.2	743.02	654.74	564.30	433.13	397.78
0.4	744.24	653.82	562.79	439.83	399.33
0.6	-	636.91	554.97	430.33	-
0.8	-	-	551.13	435.56	-

Ideally crystal should have perfect fit of atoms or molecules associated with every lattice point. Such crystal represents highest possible symmetry, however in real crystals, crystal lattice undergoes expansion or contraction depending on the size of the atoms or molecules associated with lattice points. This causes reduction in symmetry. The lowering of symmetry may split degenerate vibrations and activate inactive vibrations [30]. The cations on tetrahedral sites (formed by oxygen anions) of a cubic spinel crystal can split an absorption band into two or three bands because of site effect that lowers symmetry. The extent of this effect depends on nature of the cation and concentration [20]. So in order to incorporate substantially larger metal cations, tetrahedral sites will undergo stronger expansion compared to octahedral sites. Therefore symmetry lowering of cubic spinel crystal due to tetrahedral cations will be more than that due to cations on octahedral sites. The splitting of primary absorption band ν_1 is more intense for high Mn content; it decreases rapidly with increase in zinc content. This can be explained by the nature of tetrahedral bond. Its point symmetry is cubic (43m) and A site tetrahedral in spinel structure are isolated from each other by sharing corners with neighboring B-octahedra. No edge occurs between A site and the other A or B site polyhedra, giving rise to the single mode behavior of solid solution [31]. Hence splitting rapidly reduces with increase in zinc content. The presence of Fe^{2+} ions on octahedral sites can cause Jahn-Teller effect due to local deformation in the lattice caused by non-cubic components of the crystal field potential. Thus ν_2 band for samples $x=0.2$ and 0.4, can be assigned to $Fe^{2+}-O^{2-}$ octahedral complexes [32].

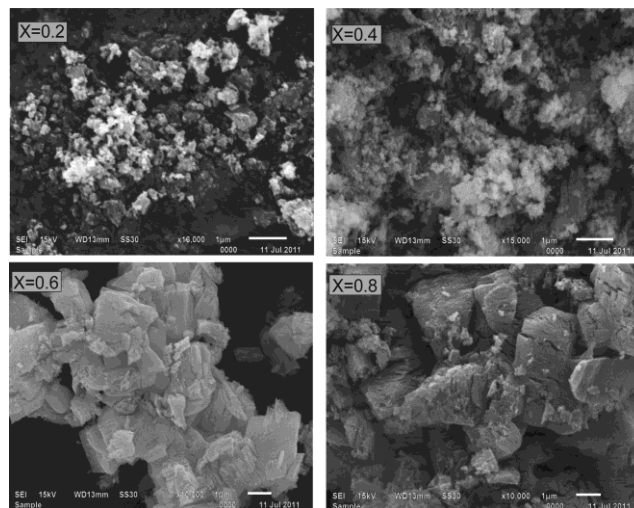


Fig. 3. Scanning electron microphotographs of $Mn_{1-x}Zn_xFe_2O_4$.

All the samples have identical morphology analyzed by scanning electron microscopy. **Fig. 3** contains four diverse representative panels of the samples under investigation. The nanocrystalline particles are observed in top panels. The partial agglomeration is due to slow particle growth in co-precipitation process. The lower panels confirm containment of large and hard agglomerates of strongly connected aggregates and individual ferrite particles in powders. These aggregates consist of nanocrystalline particles. The grain growth did not take place because the temperature of synthesis of ferrites did not exceed 450⁰ C. This work uses Aluminum powder as susceptor rather than SiC because SiC is strong absorber of microwave radiations and hence rapidly heats the samples whereas metal powders are moderate absorbers of microwave radiation, which allows easy temperature control. This facilitates that the work remains well within the nanoscale range.

Conclusion

Nanocrystalline Mn-Zn Ferrites were successfully synthesized at 450⁰ C by oxalate co-precipitation technique followed by microwave heating. Microwave synthesis saves energy and accelerates formation of ferrites since it takes only few minutes to prepare ferrites. XRD analysis confirmed the formation of single phase cubic spinel structure with crystallite sizes varying from 11 nm to 30 nm. The lattice constant is high for x = 0.2. It decreases for x = 0.4 and then gradually increases with increase in zinc content. FT-IR spectra show substantial splitting of primary absorption bands ν_1 and ν_2 . The splitting of ν_1 is due to lowering of symmetry of cubic crystalline structure of spinel ferrites. The splitting of ν_1 decreases with increase in zinc content and vanishes completely for Mn_{0.2}Zn_{0.8}Fe₂O₄. The band ν_1 shifts towards the higher wavenumber with increasing zinc content. In contrast, the splitting of ν_2 is attributed to Jahn teller distortion at octahedral site. Scanning electron microscopy confirmed formation of nanoscale particles with some agglomeration. This method can be applied for preparation of nanocrystalline materials which use microwave transparent precursors.

Acknowledgements

The Authors thank Dr. Sandeep Jasyal, Sperm Station, Palampur, India for support. The authors also thank to Apar industries limited, Baddi, India for providing High Alumina bricks free of cost.

Reference

- Priyadharsini, P.; Pradeep, A.; Sambasiva Rao, P. S.; Chandrasekaran, G.; *Mater. Chem. Phys.* **2009**, 116, 207.
DOI: [10.1016/j.matchemphys.2009.03.011](https://doi.org/10.1016/j.matchemphys.2009.03.011)
- Kaiser, M.; *J. Alloys Compd.* **2009**, 468, 15.
DOI: [10.1016/j.jallcom.2008.01.070](https://doi.org/10.1016/j.jallcom.2008.01.070)
- Feder, M.; Diamandescu, L.; Bibicu, I.; Caltun, O. F.; Dumitru, I.; Boutiuc, L.; Chiriac, H.; Lupu, N.; Vilceanu, V.; Vilceanu, M. *IEEE Trans. Magn.* **2008**, 44, 2936.
DOI: [10.1109/TMAG.2008.2002200](https://doi.org/10.1109/TMAG.2008.2002200)
- Thakur, A.; Thakur, P.; Hsu, J-H. *IEEE Trans. Magn.* **2011**, 47, 4336.
DOI: [10.1109/TMAG.2011.2156394](https://doi.org/10.1109/TMAG.2011.2156394)
- Kumar, L.; Kar, M. *IEEE Trans. Magn.* **2011**, 47, 3645.
DOI: [10.1109/TMAG.2011.2151841](https://doi.org/10.1109/TMAG.2011.2151841)
- Yu, S. H.; Fujino, T.; Yoshimura, M. *J. Magn. Magn. Mater.* **2003**, 256, 420.
DOI: [10.1016/S0304-8853\(02\)00977-0](https://doi.org/10.1016/S0304-8853(02)00977-0)
- Xin, Z.; Zhi-Ling, H.; Feng, L.; Xin, Q. *Chinese Phys. Lett.* **2010**, 27, 117501.
DOI: [10.1088/0256-307X/27/11/117501](https://doi.org/10.1088/0256-307X/27/11/117501)
- Liu, J.; He, H.; Jin, X.; Hao, Z.; Hu, Z. *Mater. Res. Bull.* **2001**, 36, 2357.
DOI: [10.1016/S0025-5408\(01\)00722-X](https://doi.org/10.1016/S0025-5408(01)00722-X)
- Barati, M. R.; Ebrahimi, S. A. S.; Dehghan, R. *IEEE Trans. Magn.* **2009**, 45, 2561.
DOI: [10.1109/TMAG.2009.2018885](https://doi.org/10.1109/TMAG.2009.2018885)
- Fu, C. W.; Syue, M. R.; Wei, F. J.; Cheng, C. W.; Chou, C. S.; *J. Appl. Phys.* **2010**, 107, 09A519.
DOI: [10.1063/1.3337689](https://doi.org/10.1063/1.3337689)
- Kim, C. W.; Koh, J. G. *J. Korean. Phys. Soc.* **2002**, 41, 364.
- Razzitte, A. C.; Jacobo, S.; Fano, W. G. *J. Appl. Phys.* **2000**, 87, 6232.
DOI: [10.1063/1.372664](https://doi.org/10.1063/1.372664)
- Date, S. K.; Joy, P. A.; Kumar, P. S. A.; Sahoo, B.; Keunne, W. *Phys. Status Solidi (c)* **2004**, 1, 3495.
DOI: [10.1002/pssc.200405489](https://doi.org/10.1002/pssc.200405489)
- Ewais, E. M. M.; Hessein, M. M.; El-Geassy, A. H. A. *J. Australian. Ceram. Soc.* **2008**, 44, 57.
- Janasi, S. R.; Rodrigues, D.; Landgraf, F. J. G.; Emura, M. *IEEE Trans. Magn.* **2000**, 36, 3327.
DOI: [10.1109/20.908788](https://doi.org/10.1109/20.908788)
- Mathur, P.; Thakur, A.; Singh, M. *J. Mater. Sci.* **2007**, 42, 8189.
DOI: [10.1007/s10853-007-1690-y](https://doi.org/10.1007/s10853-007-1690-y)
- Rao, B. P.; Caltun, O. F. *J. Optoelectron. Adv. Mater.* **2006**, 8, 991.
- Mathew, D. S.; Juang, R. S. *Chem. Eng. J.* **2007**, 129, 51.
DOI: [10.1016/j.cej.2006.11.001](https://doi.org/10.1016/j.cej.2006.11.001)
- Li, L.; Lan, Z.; Yu, Z.; Sun, K.; Xu, Z.; Ji, H. *IEEE Trans. Magn.* **2008**, 44, 2107.
DOI: [10.1109/TMAG.2008.2000809](https://doi.org/10.1109/TMAG.2008.2000809)
- Hu, P.; Yang, H.; Pan, D.; Wang, H.; Tian, J.; Zhang, S.; Wang, X.; Volinsky, A. A. *J. Magn. Magn. Mater.* **2010**, 322, 173.
DOI: [10.1016/j.jmmm.2009.09.002](https://doi.org/10.1016/j.jmmm.2009.09.002)
- Kashyap, S. C. *Applied electromagnetic conference* **2009**, 1.
DOI: [10.1109/AEMC.2009.5430602](https://doi.org/10.1109/AEMC.2009.5430602)
- Panapoy, M.; Supattanapalapol, S.; Ksapabutr, B. *2nd IEEE International Nanoelectric conference* **2008**, 452.
DOI: [10.1109/INEC.2008.4585456](https://doi.org/10.1109/INEC.2008.4585456)
- Joshi, U. A.; Jang, J. S.; Borse, P. H.; Lee, J. S. *Appl. Phys. Lett.* **2008**, 92, 242106.
DOI: [10.1063/1.2946486](https://doi.org/10.1063/1.2946486)
- Microwave processing of materials. National academy Press, Washington d.c. 1994; 7-29.
- Wang, Z. L.; Liu, Y.; Zhang, Z. *Handbook of Nanophase and Nanostructured Materials: Synthesis*, Springer **2002**, 67.
- Cushing, B.; Vladimir, b. I.; Kolesnihenko, V.; O'Connor, C. J. *Chem Rev.* **2004**, 104, 3893.
DOI: [10.1021/cr030027b](https://doi.org/10.1021/cr030027b)
- Gopalan, E. V.; Malini, K. A.; Kumar, D. S.; Saravanan, S.; Yoshida, Y.; Anantharaman, M. R. *J. Phys. D: Appl. Phys.* **2008**, 41, 18005.
DOI: [10.1088/0022-3727/41/18/185005](https://doi.org/10.1088/0022-3727/41/18/185005)
- Modi, K. B.; Rangolia, M. K.; Chhantbar, M. C.; Joshi, H. H. *J. Mater. Sci.* **2006**, 41, 73008.
DOI: [10.1007/s10853-006-0929-3](https://doi.org/10.1007/s10853-006-0929-3)
- Waldron, R. D. *Phys. Rev.* **1955**, 99, 1727.
DOI: [10.1103/PhysRev.99.1727](https://doi.org/10.1103/PhysRev.99.1727)
- Nakamoto, K. *Infrared and Raman spectra of Inorganic and coordination compounds*. 6th Edition, Part A. John Wiley and Sons, **2009**, 119.
- Salah, L. M. *Phys. Status Solidi (a)* **2006**, 203, 271
DOI: [10.1002/pssa.200521285](https://doi.org/10.1002/pssa.200521285).
- Zaki, H. M.; Dawoud, H. A. *Physica B cond. Mat.* **2010**, 405, 4476.
DOI: [10.1016/j.physb.2010.08.018](https://doi.org/10.1016/j.physb.2010.08.018)

Advanced Materials Letters

Publish your article in this journal

ADVANCED MATERIALS Letters is an international journal published quarterly. The journal is intended to provide top-quality peer-reviewed research papers in the fascinating field of materials science particularly in the area of structure, synthesis and processing, characterization, advanced-state properties, and applications of materials. All articles are indexed on various databases including DOAJ and are available for download for free. The manuscript management system is completely electronic and has fast and fair peer-review process. The journal includes review articles, research articles, notes, letter to editor and short communications.

